Since January 2020 Elsevier has created a COVID-19 resource centre with free information in English and Mandarin on the novel coronavirus COVID-19. The COVID-19 resource centre is hosted on Elsevier Connect, the company's public news and information website.

American Society of Hematology
2021 L Street NW, Suite 900,
Washington, DC 20036
Phone: 202-776-0544 | Fax 202-776-0545
editorial@hematology.org

The Histone Methyltransferase MLL1/KMT2A in Monocytes Drives Coronavirus-Associated Coagulopathy and Inflammation

Tracking no: BLD-2022-015917R2

Sriganesh Sharma (University of Michigan, United States) William Melvin (University of Michigan, United States) Christopher Audu (University of Michigan, United States) Monica Bame (University of Michigan, United States) Nicole Rhoads (University of Michigan, United States) Weisheng Wu (University of Michigan, United States) Yogendra Kanthi (National Institutes of Health, United States) Jason Knight (University of Michigan, United States) Reheman Adili (University of Michigan, United States) Michael Holinstat (University of Michigan, United States) Thomas Wakefield (University of Michigan, United States) Peter Henke (University of Michigan, United States) Bethany Moore (University of Michigan, United States) Katherine Gallagher (University of Michigan, United States) Andrea Obi (University of Michigan, United States)

Abstract:
Coronavirus-associated coagulopathy (CAC) is a morbid and lethal sequela of SARS-CoV-2 infection. CAC results from a perturbed balance between coagulation and fibrinolysis and occurs in conjunction with exaggerated activation of monocytes/macrophages (MO/Mφs) and the mechanisms that collectively govern this phenotype seen in CAC remain unclear. In this study, using experimental models that employ the murine betacoronavirus MHVA59, a well-established model of SARS-CoV-2 infection, we identify that the histone methyltransferase Mixed Lineage Leukemia 1 (MLL1/KMT2A) is an important regulator of MO/Mφ expression of procoagulant and profibrinolytic factors such as tissue factor (F3; TF), urokinase (PLAU), and urokinase receptor (PLAUR) (herein "coagulopathy-related factors") in non-infected and infected cells. We show that MLL1 concurrently promotes the expression of the proinflammatory cytokines while suppressing the expression of interferon a (IFNa), a well-known inducer of TF and PLAUR. Using *in vitro* models, we identify MLL1-dependent NFκB/RelA-mediated transcription of these coagulation-related factors and identify a context dependent MLL1-independent role for RelA in the expression of these factors *in vivo*. As functional correlates for these findings, we demonstrate that the inflammatory, procoagulant and profibrinolytic phenotypes seen *in vivo* after coronavirus infection were MLL1-dependent despite blunted *Ifna* induction in MO/Mφs. Finally, in an analysis of SARS-CoV-2 positive human samples, we identify differential upregulation of MLL1 and coagulopathy-related factor expression and activity in $CD14^+$ MO/Mφs relative to non-infected and healthy controls. We also observed elevated plasma urokinase and TF activity in COVID-positive samples. Collectively, these findings highlight an important role for MO/Mφ MLL1 in promoting coronavirus-associated coagulopathy and inflammation.

Conflict of interest: COI declared - see note

COI notes: M.H. is a consultant and equity holder for Veralox Therapeutics and a consultant for Cereno Scientific which has an option to license platelet inhibitory compounds from the University of Michigan. The authors do not have any conflicts of interest to declare otherwise.

Preprint server: No;

Author contributions and disclosures: S.B.S., W.J.M., C.A.O., M.B., N.R., Y.K., J. S. K., R.A., M.H., B.B.M., P.K.H., T. W. W., K.A.G. and A.T.O. designed research strategy; S.B.S., W.J.M., C.O.A., M.B., N.R., and A.T.O. performed research; S.B.S., W.J.M., C.A.O., W.W., N.R., R.A., M.H., B.B.M, P.K.H, K.A.G., and A.T.O. contributed new reagents/analytic tools; W.W. performed analysis of sequencing data; S.B.S., W.J.M., C.A.O., N.R., R.A., M.H., B.B.M., T.W.W., P.K.H., K.A.G, and A.T.O. analyzed data; S.B.S and A.T.O. wrote the paper.

Non-author contributions and disclosures: No;

Agreement to Share Publication-Related Data and Data Sharing Statement: For original data, please contact Dr. Andrea Obi (easta@med.umich.edu)

Clinical trial registration information (if any):

The Histone Methyltransferase MLL1/KMT2A in Monocytes Drives Coronavirus-Associated Coagulopathy and Inflammation

Monocyte MLL1 drives COVID-Associated Coagulopathy

Sriganesh B. Sharma[1]; William J. Melvin[1]; Christopher O. Audu[1,2]; Monica Bame[3]; Nicole Rhoads[4]; Weisheng Wu[5]; Yogendra Kanthi[6]; Jason S. Knight[7]; Reheman Adili[4]; Michael Holinstat[2,4]; Thomas W. Wakefield[1,2]; Peter K. Henke[1,2]; Bethany B. Moore[3]; Katherine A. Gallagher[1,2,3]; Andrea T. Obi[1,2*]

[1]Department of General Surgery, University of Michigan, Ann Arbor, Michigan; [2]Section of Vascular Surgery, Department of Surgery, Ann Arbor, Michigan; [3]Department of Microbiology and Immunology, University of Michigan, Ann Arbor, Michigan; [4]Department of Pharmacology, University of Michigan, Ann Arbor, Michigan; [5]Bioinformatics core, Biomedical research core facilities, University of Michigan, Ann Arbor, Michigan; [6]Laboratory of Vascular Thrombosis & Inflammation, National Heart, Lung, and Blood Institute, Bethesda, Maryland; [7]Division of Rheumatology, Department of Internal Medicine, University of Michigan, Ann Arbor, Michigan;

[*]**Corresponding author:** Dr. Andrea T. Obi, MD; easta@med.umich.edu

Word counts for text/abstract: 4000 for text (introduction, materials & methods, results, and discussion; including headings); 250 for abstract

Figure count: 7 main, 24 supplemental

Table count: 0 main, 8 supplemental

Reference count:

Key Points:

- Monocyte/Macrophage MLL1 promotes the expression of coagulopathy-related factors and proinflammatory cytokines after coronavirus infection
- Loss of monocyte/macrophage MLL1 attenuates the profibrinolytic and thrombophilic phenotype observed upon coronavirus infection *in vivo*

Abstract:

Coronavirus-associated coagulopathy (CAC) is a morbid and lethal sequela of SARS-CoV-2 infection. CAC results from a perturbed balance between coagulation and fibrinolysis and occurs in conjunction with exaggerated activation of monocytes/macrophages (MO/Mφs) and the mechanisms that collectively govern this phenotype seen in CAC remain unclear. In this study, using experimental models that employ the murine betacoronavirus MHVA59, a well-established model of SARS-CoV-2 infection, we identify that the histone methyltransferase Mixed Lineage Leukemia 1 (MLL1/KMT2A) is an important regulator of MO/Mφ expression of procoagulant and profibrinolytic factors such as tissue factor (F3; TF), urokinase (PLAU), and urokinase receptor (PLAUR) (herein "coagulopathy-related factors") in non-infected and infected cells. We show that MLL1 concurrently promotes the expression of the proinflammatory cytokines while suppressing the expression of interferon α (IFNα), a well-known inducer of TF and PLAUR. Using *in vitro* models, we identify MLL1-dependent NFκB/RelA-mediated transcription of these coagulation-related factors and identify a context dependent MLL1-independent role for RelA in the expression of these factors *in vivo*. As functional correlates for these findings, we demonstrate that the inflammatory, procoagulant and profibrinolytic phenotypes seen *in vivo* after coronavirus infection were MLL1-dependent despite blunted *Ifna* induction in MO/Mφs. Finally, in an analysis of SARS-CoV-2 positive human samples, we identify differential upregulation of MLL1 and coagulopathy-related factor expression and activity in $CD14^+$ MO/Mφs relative to non-infected and healthy controls. We also observed elevated plasma urokinase and TF activity in COVID-positive samples. Collectively, these findings highlight an important role for MO/Mφ MLL1 in promoting coronavirus-associated coagulopathy and inflammation.

Introduction:

Infection with SARS-CoV-2 results in physiologic derangements that stem from both the direct action of viral infection and ensuing host-immune response[1,2]. Among these sequalae is COVID-associated coagulopathy (CAC), which results in increased thrombotic complications and mortality, and features low-grade disseminated intravascular coagulopathy and thrombotic microangiopathy[3-5]. The underlying pathophysiology is related in part to the combined actions of opposing processes including thromboinflammation[6,7] and altered fibrinolysis due to the activity of urokinase (PLAU) and urokinase receptor (PLAUR), which results in D-dimer elevation that correlates with disease severity[3,8-11]. The concurrent increased risk of arterial and venous micro/macrothrombosis, represents a major unaddressed cause of SARS-CoV-2 morbidity and mortality[2,12].

The pathophysiology of CAC involves exaggerated activation of leukocytes (including monocytes/macrophages [MO/Mφs]), endothelial cells, and platelets[2,13-16]. MO/Mφs impact local and systemic coagulation and fibrinolysis via expression of tissue factor (F3; TF), PLAU, and PLAUR ("coagulopathy-related factors") in response to various stimuli, including coronavirus infection, and inflammatory cytokine and interferon/interferon receptor (IFN/IFNR) stimulation[17-24]. The stimuli that govern MO/Mφ responsiveness to SARS-CoV-2 infection are not well understood but may be related to patient factors[25], alterations in IFN response[26,27], or epigenetic regulation by chromatin modifying enzymes (CMEs) and associated proteins[28,29]. CMEs alter MO/Mφ function and are implicated in a variety of disease contexts including wound healing[30-32], atherosclerosis[33,34], and aneurysm development[35], and affect cytokine response in diabetic patients after SARS-CoV-2 infection[29]. Importantly, epigenetic changes may induce long-lasting alterations in gene expression ("epigenetic memory") following acute infection and may facilitate long term sequelae seen after coronavirus infection[28,36].

A candidate CME in altering MO/Mφ function is the histone methyltransferase Mixed Lineage Leukemia 1 (MLL1/KMT2A), which is ubiquitously expressed in human tissues[37], functions in core complexes containing accessory proteins such as WDR5[38,39] and Menin[40], and catalyzes the addition of methyl-groups to lysine-4 residues on histone 3 proteins and facilitates a chromatin conformation conducive for gene transcription[41]. Initially recognized for its role in leukemogenesis[42], MLL1 has recently emerged as an important driver of MO/Mφ response in many disease states[30,31,36,43,44]. Previous work demonstrates MLL1-mediated IL1β expression and implicates epigenetic changes secondary to MLL1 suppression in MO/Mφs following recovery from sepsis that impact wound healing[36]. MLL1 plays critical roles in facilitating immune responses downstream of proinflammatory and type I

IFN signaling pathways involving IL6, TNFα, and STAT4[45,46]. MLL1 is also important in orchestrating signaling involving NFκB activation[47], which occurs through activation RelA, and is induced by SARS-CoV-2 infection. Since RelA and IFN signaling regulate inflammatory cytokine and coagulopathy-related factor expression[24,26,48-50], we postulated that MLL1 may impact the expression of these factors in MO/Mφs to promote coagulopathy and systemic inflammation.

To this end, we utilized the murine betacoronavirus MHVA59 (a well-established model of SARS-CoV-2 infection[29,51]) to across *in vitro* and *in vivo* models to study the role of MLL1 in regulating the expression of CAC-related factors, inflammatory cytokines and IFN/IFNRs. We found that infection of MO/Mφs yielded induction of MLL1, coagulopathy-related factors, and cytokines. Through loss-of-function models, we identified that the transcription of MLL1, these factors, and cytokines was directly regulated by MLL1. Next, we demonstrated that MLL1 is required for RelA-dependent transcription of coagulopathy-related factors *in vitro*. We showed that MLL1 is critical in inducing MO/Mφ and plasma expression of these factors and cytokines in response to coronavirus infection and in promoting a prothrombotic/profibrinolytic phenotype *in vivo*. Interestingly, loss of MO/Mφ MLL1 de-repressed expression of *Ifna*, a mediator of coagulopathy in other contexts[26], despite attenuating coronavirus-induced coagulopathy. Finally, we observed upregulated MO/Mφ MLL1, coagulopathy-related and inflammatory cytokine expression in $CD14^+$ MO/Mφs and plasma derived from COVID-positive patients, who also displayed a concurrent induction of plasma urokinase and TF activity. Collectively, these results implicate MLL1 as a driver of MO/Mφ signaling critical for coronavirus-associated coagulopathy and inflammation.

Materials and Methods:

Animals and MHVA59 inoculation: C57BL6/J mice were obtained from The Jackson Laboratory and *Kmt2a*$^{fl/fl}$Lyz2Cre$^{+/-}$ and *Kmt2a*$^{fl/fl}$Lyz2Cre$^{-/-}$ mice were generated as previously described[36]. MHVA59 was generated as described previously[29]. Mice underwent intranasal inoculation of $2x10^5$ plaque forming units of MHVA59 or with phosphate buffered saline. Animal studies were performed with the approval of the University of Michigan institutional animal care and use committee.

Tail bleeding assays and Thromboelastography (TEG): Mice were anesthetized using ketamine/xylazine and placed on a heating pad. Five millimeters of the tail tip was sharply excised, and the tail was immersed in saline at 37^{o}C. Bleeding time was defined as cessation of bleeding for 1 minute. Re-bleeds were identified if bleeding

occurred within the 10-minute observation period for each animal. For TEG, whole blood was drawn from the inferior vena cava and citrate-anticoagulated (1:9; 3.2% sodium citrate:whole blood). 340µl of anticoagulated blood was mixed with 20µl of 0.2N $CaCl_2$ and viscoelastic properties were analyzed using the Haemoscope TEG 5000 Thrombelastograph Hemostasis Analyzer (Haemonetics Corp.). Where indicated, corn trypsin inhibitor (CTI; Prolytix) or TF-inhibiting antibody (TFI; rat-anti-mouse IgG2a/κ clone 1H1; Genentech) was incubated with anticoagulated whole blood for 15 minutes at 37^{o}C prior to TEG. Plasma was obtained by centrifugation of whole blood at 2,000g for 10 minutes for two sequential spins.

Human samples: Plasma/buffy coats were isolated from peripheral blood samples collected from hospitalized COVID-positive and COVID-negative patients, and healthy controls by centrifugation of citrate-anticoagulated whole blood specimens for two sequential spins at 2000*g* for 15 min at room temperature. Patient characteristics are listed in Supplemental Table 8. $CD14^{+}$ MO/Mφs were isolated using the EasySep Human CD14 Positive Selection Kit (Stemcell Technologies). All samples were collected under approved protocols from the University of Michigan Institutional Review Board.

Supplemental methods: A detailed description of other methods is provided in the supplement.

Data sharing statement: For original data, please contact Andrea Obi (easta@med.umich.edu).

Results:

Coronavirus infection of MO/Mφs induces MLL1, coagulopathy-related factors, inflammatory cytokines, type I-III IFN/IFNRs.

Previous studies demonstrate that inflammatory MO/Mφ activation occurs in an MLL1-dependent fashion[30,31,34,36]. Therefore, we chose to investigate if MLL1 expression was increased in Mφs in response to coronavirus infection. We performed infection of bone marrow derived Mφs (BMDMs) derived from C57BL6/J mice with murine coronavirus MHVA59. Infected BMDMs displayed induction of MLL1 expression relative to non-infected cells (Figures 1A-B). We observed similar upregulation of coagulopathy-related factor and inflammatory cytokine expression (Figures 1C-F) in BMDMs and in a second context which utilized immortalized murine Mφs (RAW264.7; Supplemental Figure 1). Additionally, we observed induction of mRNA levels of types I-III IFNs and IFNRs in BMDMs (Supplemental Figure 2) in response to coronavirus infection. These results identify

MLL1, the coagulopathy-related factors PLAU, PLAUR, and F3, the inflammatory cytokines IL6, IL1β, and TNFα, and type I-III IFNs as coronavirus-inducible factors *in vitro*.

MLL1 regulates basal expression of coagulopathy-related factors, inflammatory cytokines, and type I IFNs and type III IFNRs in MO/Mφs.

As MLL1 has been described to regulate inflammatory gene and type I IFN-dependent responses after TLR ligand and/or cytokine stimulation[31,45], we queried whether MLL1 was responsible for the expression of coagulopathy-related factors, inflammatory cytokines, and IFN/IFNR genes in MO/Mφs in the non-infected state. We analyzed expression of these genes in BMDMs from mice with myeloid specific MLL1 knockout (*Kmt2a*$^{fl/fl}$Lyz2Cre$^{+/-}$; denoted Cre+) and littermate controls (*Kmt2a*$^{fl/fl}$Lyz2Cre$^{-/-}$; denoted Cre-). We confirmed loss of MLL1 in harvested BMDMs (Figures 2A-B) and observed attenuated expression (Figures 2C-F) of coagulopathy-related factors and inflammatory cytokines in Cre+ BMDMs relative to Cre- cells. Furthermore, we observed MLL1-dependent H3K4me3 abundance on the promoters of coagulopathy-related factors (Figure 2G). Interestingly, denoting MLL1 self-regulation, MLL1 loss resulted in attenuated H3K4me3 abundance at its own promoter (Figure 2G). Moreover, baseline MLL1 promoter occupancy at candidate promoters in Cre- cells was observed, and as expected, this occupancy was lost in Cre+ cells (Supplemental Figure 3A). Finally, we observed MLL1-dependent occupancy of phosphorylated RNA polymerase II β-subunit (Ser5; phospho-Rpb1), a marker of active transcription, at the promoters of coagulopathy-related factors (Supplemental Figure 3B). These results indicate that MLL1 promotes the transcription of coagulopathy-related factors and itself.

We observed an induction of type I IFN (*Ifna* and *Ifnb1*) and type III IFNR levels in Cre+ cells compared to Cre- cells (Supplemental Figure 4), and these results indicated a role for MLL1 in regulating basal IFN signaling and responsiveness *in vitro*. We observed similar MLL1-dependent regulation after siRNA-mediated MLL1 silencing in WT-BMDMs (Supplemental Figure 5-6) and RAW264.7 cells (Supplemental Figure 7). Collectively, these results identify basal MLL1-dependent regulation of coagulopathy-related factors and inflammatory cytokines in MO/Mφs.

MLL1 regulates coronavirus and inflammatory cytokine-dependent induction of coagulopathy-related factors and inflammatory cytokines.

In contrast to SARS-CoV-2, MHVA59 employs CEACAM1[52,53] (found on murine MO/Mφs) as a co-receptor for cell entry. Therefore, we sought to determine whether MLL1 mediated either MHVA59-initiated or MHVA59-independent induction of coagulopathy-related factors and inflammatory cytokines. We stimulated Cre- and Cre+ BMDMs with either cytokines induced in the post-coronavirus hyperimmune state[54-56] or with MHVA59. We observed robust induction of coagulopathy-related factors and inflammatory cytokines after stimulation with each cytokine and MHVA59 infection in Cre- cells (Figures 3A-D). A notable exception was that the PLAU levels were suppressed by IL6 stimulation, and this finding indicated heterogeneity of cellular responses to inflammatory stimuli. We also observed MLL1-dependent enrichment of H3K4me3, MLL1, and phospho-Rpb1 on the promoters of MLL1 and coagulopathy-related factors after cytokine/coronavirus stimulation (Figure 3E, Supplemental Figures 8A-B). Collectively, these results highlight an important role for MLL1 in cytokine/coronavirus-mediated induction of coagulopathy-related factors and inflammatory cytokines. We confirmed our findings in MLL1-silenced BMDMs (Supplemental Figure 9) and RAW264.7 cells (Supplemental Figure 10).

MLL1 alters IFN production and IFN-dependent coagulopathy-related factor expression in BMDMs.

As type I interferons such as IFNα have been described to promote coagulopathy through the expression PLAUR[24] and F3[57], and the dysregulation of IFN signaling has been implicated in the pathogenesis of SARS-CoV-2 sequelae[26,58,59], we chose to determine the role of MLL1 in mediating IFN production and responsiveness after coronavirus infection. We observed that Cre+ BMDMs displayed an induction of *Ifna*, *Ifnar1*, *Ifngr1*, and type III IFN/IFNR mRNA expression, but also a suppression of *Ifng* levels after coronavirus infection (Supplemental Figure 11). Interestingly, though only IFNα1 and IFNγ stimulation induced *Kmt2a* expression (Supplemental Figure 12A), only IFNα1 stimulation yielded enhanced expression of coagulopathy-related factors, and this induction was blunted in Cre+ cells (Supplemental Figures 12B-D). These results highlight a dominant role for MLL1 in regulating IFNα/coagulopathy-related-factor signaling after coronavirus infection *in vitro*.

MLL1 is required for RelA-dependent transcription of coronavirus-responsive factors.

As MLL1 function has been previously shown to be influenced by NFκB signaling[47], we chose to investigate collaborative gene regulation by MLL1 and RelA in MO/Mφs. We did not observe altered levels of RelA mRNA or protein levels in Cre+ BMDMs relative to Cre- BMDMs (Figures 4A-B). Since activated RelA (phosphorylated on Ser276 or Ser536) protein levels were not readily detectable in BMDMs in the basal state, we

analyzed RAW264.7 cells and did not observe any differences in phospho-RelA levels upon MLL1 knockdown (Figure 4C). Conversely, we did not observe RelA-mediated regulation of MLL1 expression in siRelA treated BMDMs (Figures 4D-E). However, MHVA59 infection of RelA-silenced BMDMs yielded attenuated induction of MLL1 (Figure 4F), though RelA levels were not induced in either Cre- or Cre+ cells (Figure 4G). Collectively, these results identify that RelA is needed for maximal induction of MLL1 levels after coronavirus infection and that RelA and MLL1 do not participate in reciprocal regulation of each other's expression in MO/Mφs in the basal state.

Following coronavirus infection, we observed increased time-dependent RelA occupancy at the *Kmt2a* promoter (Figure 4H). The ability of RelA to occupy the MLL1 promoter was dependent on MLL1 expression as attenuated promoter occupancy dynamics were observed in Cre+ cells. We also observed that though RelA silencing alone yielded a modest suppression of the coagulopathy-related factor and inflammatory cytokine expression in response to MHVA59 infection (Figures 4I-J, Supplemental Figures 13A-B), combined RelA and MLL1 loss resulted in robust abrogation of the coronavirus-dependent induction of these genes. Similarly, RelA abundance at the coagulopathy-related factor promoters was attenuated in Cre+ BMDMs that were infected with MHVA59 (Figure 4K). Collectively, these results show that MLL1 is required for RelA-dependent transcription of coagulopathy-related factors and inflammatory cytokines in MO/Mφs *in vitro*.

Coronavirus infection results in induction of MLL1 and dependent factors *in vivo.*

We next aimed to determine whether MLL1 and its dependent factors are induced in MO/Mφs upon coronavirus infection *in vivo*. C57BL6/J mice underwent intranasal inoculation of either $2x10^5$ *pfu* of MHVA59 or with PBS (sham). Through viral PCR and MHVA59 enumeration assays, we determined that post-infection day 3 (d3) represented a period of robust viremia and infection of lung, splenic MO/Mφs, and BMDMs and that post-infection day 28 (d28) represented a late timepoint during which no measurable virus was present in these tissues (Supplemental Figure 14). MHVA59 infection induced the expression of MLL1, coagulation-related factors, and inflammatory cytokines (Figures 5A-C, Supplemental Figures 15A-B). Concordant with our *in vitro* findings, we observed induction of H3K4me3, MLL1, and RelA occupancy on the promoters of *Kmt2a* and the coagulopathy-related factors (Figure 5D and Supplemental Figures 15C-D). Interestingly, MLL1 silencing in splenic MO/Mφs harvested from infected animals was able to attenuate coronavirus-mediated gene expression (Supplemental Figure 16). However, compared to our *in vitro* studies (Supplemental Figure 2), we observed that splenic MO/Mφs

displayed suppressed levels of *Ifnar1* and type II IFN/IFNRs, despite displaying inductions in *Ifna* and type III IFN/IFNRs (Supplemental Figure 17). Nonetheless, we observed similar coagulopathy-related and inflammatory cytokine gene expression and epigenetic changes in BMDMs from infected animals (Supplemental Figure 18).

Finally, we observed coronavirus-mediated induction of plasma inflammatory cytokine and coagulopathy-related factor expression (Supplemental Figure 15E and Figures 5), and soluble PLAU/PLAUR expression (Figures 5E-G). We also observed an induction in plasma urokinase activity, and plasma and MO/Mφ TF activity, suggesting a concurrent fibrinolytic and hypercoagulable phenotype (Figures 5H-J). To explore functional consequences of these results, we performed tail bleeding assays and thromboelastography (TEG). Coronavirus infection resulted in faster cessation of tail bleeding and predisposed animals to a higher rate of re-bleeding, thus demonstrating a hypercoagulable phenotype in which clot stability dynamics were perturbed, possibly through hyperfibrinolysis (Figures 5K-L). Using TEG, we observed that coronavirus infection yielded shortened clot formation times (R) (Figure 5M). We attributed this observation to TF activity as we observed a preferential effect of corn trypsin inhibitor treatment (inhibitor of intrinsic coagulation)[60] in prolonging R-times in samples from sham animals (Figure 5N). Furthermore, treatment of samples with 100 μg/ml, but not 50 μg/ml of murine specific TF blocking antibody[61] (TFI) was required to abrogate clot formation in infected samples, whereas 50 μg/ml of TFI was sufficient to block clot formation in sham samples (Figure 5N). Collectively, these results show that the expression of MLL1, coagulation-related factors, and inflammatory cytokines is induced in an MLL1-dependent manner *in vivo* in response to coronavirus infection and culminates in a prothrombotic and hyperfibrinolytic phenotype.

MLL1 loss in MO/Mφs attenuates coronavirus-mediated induction of coagulation-related factors and inflammatory cytokines *in vivo*.

To further demonstrate MLL1-dependency for the induction of coagulation-related factors and inflammatory cytokines, we performed inoculation of Cre- and Cre+ mice with MHVA59. We observed robust induction of levels of coagulopathy-related factors and inflammatory cytokines in harvested Cre- BMDMs (Supplemental Figures 19A-B) and splenic MO/Mφs compared to Cre+ cells (Figures 6A-B and Supplemental Figures 20A-B). We also observed differentially induced H3K4me3 enrichment on the promoters *of Kmt2a* and the coagulopathy-related factors in Cre- splenic MO/Mφs and BMDMs relative to Cre+ cells upon coronavirus infection (Figure 6C; Supplemental Figure 19C). However, we did not observe MLL1-dependence of RelA occupancy in

284 splenic MO/Mφs or differential promoter occupancy of RelA in BMDMs (Supplemental Figure 20C and 19D) in
285 contrast to our results *in vitro* (Figure 4K).

286 Indicating MLL1-dependence, plasma levels of inflammatory cytokines (Supplemental Figure 20D) and
287 coagulopathy-related factors (Figures 6D-F) were differentially upregulated in infected Cre- mice. Furthermore, we
288 observed a robust increase in plasma urokinase activity, and plasma and MO/Mφ TF activity (Figures 6G-I) in Cre-
289 mice compared to Cre+ mice. Finally, infected Cre- mice displayed shortened tail bleeding times with increased re-
290 bleeding events (Figures 6J-K) and shortened R-times which were TF dependent (Figures 6L-M). Interestingly,
291 uninfected Cre- and Cre+ mice did not display such differences, suggesting a context specific role for MO/Mφ
292 MLL1 *in vivo*. These results further support MO/Mφ MLL1's role in the pathogenesis of coronavirus-dependent
293 inflammatory coagulopathy.

294 **MLL1 loss alters IFN responsiveness of MO/Mφs but does not affect MHVA59 infection *in vivo.***

295 We next chose to investigate whether MO/Mφ MLL1 impacted IFN production and responsiveness after
296 coronavirus infection *in vivo*. Analysis of type I-III IFN/IFNR mRNA transcript expression showed a consistent
297 pattern of IFN/IFNR transcript changes in splenic MO/Mφs between infected Cre- and C57Bl6/J animals
298 (Supplemental Figures 21 and 17). Interestingly, we observed concordant induction of only *Ifna* and *Ifnlr1* mRNA
299 levels in uninfected Cre+ BMDMs *in vitro* and Cre+ splenic MO/Mφs derived from sham animals *in vivo*
300 (Supplemental Figures 11 and 21). Analysis of infected BMDMs *in vitro* and splenic MO/Mφs derived from
301 infected animals also revealed concordant induction of *Ifna*, *Ifnar1*, and *Ifnlr1* in Cre+ cells compared to Cre- cells
302 (Supplemental Figures 11 and 21). Finally, a limited transcriptomic analysis by qRT-PCR array of IFN-signaling
303 relevant genes revealed heterogeneous coronavirus-mediated responses between uninfected and infected Cre- and
304 Cre+ splenic MO/Mφs (Sham: Cre+ v. Cre- MO/Mφs – decreased expression of 29/66 [43.9%, 1.25-fold average
305 decrease in expression] and increased expression of 37/66 [56.1%, 3.11-fold average increase in expression] of
306 analyzed transcripts; d3 Cre+ v. d3 Cre- MO/Mφs – decreased expression of 35/66 [53.0%, 1.73-fold average
307 decrease in expression] and increased expression of 31/66 [47.0%, 2.07-fold average increase in expression] of
308 analyzed transcripts), but nonetheless implicated *Ifna* transcripts as MLL1-repressible elements in both uninfected
309 and infected states (Supplemental Figure 21G). Despite these results in Cre- and Cre+ animals, we did not observe
310 differences in MHVA59 infection of lung, splenic MO/Mφs, BMDMs, or whole blood through viral PCR or viral

enumeration assay (Supplemental Figure 22). Thus, our results highlight MLL1-IFNα signaling that may preferentially impact coagulopathy after coronavirus infection.

MLL1 and regulated factors are induced in CD14$^+$ cells and plasma derived from SARS-CoV-2 infected patients.

We assessed whether MO/Mφs isolated from human SARS-CoV-2 positive samples displayed differential expression of MLL1 and dependent factors. We isolated CD14$^+$ MO/Mφs and peripheral plasma samples from hospitalized SARS-CoV-2 infected patients (n=28; hCoV+), hospitalized SARS-CoV-2 negative patients (n=24; hCoV-), and healthy controls (n=14) and identified elevated mRNA levels of MLL1 in hCoV+ patients compared to hCoV- patients and healthy controls (Figure 7A). We observed differential induction of MO/Mφ and plasma levels of coagulopathy-related factors in hCoV+ patients (Figures 7B-D, Supplemental Figures 23A-C). We observed these changes in coagulopathy-related factors despite suppressed *Ifna* and *Ifnb1* mRNA levels in CD14$^+$ cells from hCoV+ patients compared to hCoV- patients (Supplemental Figure 24). We also observed increased abundance of MLL1, H3K4Me3, and RelA occupancy at the promoters of MLL1 and coagulopathy-related factors in hCoV+ MO/Mφs relative to other groups (Figures 7E-F, Supplemental Figures 23C-D). Finally, we observed that elevated plasma coagulation-related factor levels corresponded with induced urokinase and TF activity (Figures 7G-H). These data mirror our experimental findings regarding MLL1 and show that hCoV+ patients display a MO/Mφ and a plasma profile featuring induced coagulopathy-related factors and inflammatory cytokines.

Discussion:

In this study, we report a critical role for MLL1 in promoting expression of coagulopathy-related factors and inflammatory cytokines after coronavirus infection and delineate a context-specific role for MLL1 in regulating RelA-dependent transcription of these factors (Figure 7I). We identify self-regulation of MLL1 expression and show that myeloid MLL1 loss attenuates coronavirus-induced hypercoagulable/profibrinolytic phenotype *in vivo* despite de-repressing expression of IFNα, which has been described as an inducer of coagulopathy after endotoxemia[57]. Finally, we demonstrate differential expression/activity of MLL1 and coagulopathy-related factors in samples from SARS-CoV-2 positive patients. These findings highlight a novel role for MO/Mφ MLL1 as a dominant regulator for the expression of factors important for CAC.

Due to differences in cell-specificity between MHVA59 (utilizes CEACAM1 as co-receptors; found on murine MO/Mφs[52,53]) and SARS-CoV-2, it is difficult to dissect MHVA59-dependent regulation of MLL1 from virus-independent mechanisms. Nonetheless, we identify inflammatory cytokine-mediated MLL1 induction and reciprocal regulation of these cytokines by MLL1. Furthermore, we demonstrate *Kmt2a* and *Plaur* as two novel MLL1/RelA-regulated targets. Though we did not identify reciprocal regulation of the expression MLL1 or RelA, we observed that MLL1 regulated RelA occupancy at the *Kmt2a*, *Plau*, *Plaur*, and *F3* promoters *in vitro* but not *in vivo*. These results across may highlight context-dependent NFκB/RelA signaling dynamics which have been described in response to variety of stimuli[62-65]. Nonetheless, we observed increased MLL1 and RELA occupancy on coagulopathy-related gene promoters in COVID-positive MO/Mφs relative to samples from COVID-negative patients and healthy controls, indicating a potential for collaborative transcriptional regulation after SARS-CoV-2 infection.

In contrast to the bidirectional regulation between MLL1 and its dependent inflammatory effectors, we observed heterogeneity in MLL1-regulated IFN expression/responsiveness across experimental contexts, though *Ifna* suppression by MLL1 was a consistent observation. This finding may explain a mechanism by which type I IFN expression/responses are repressed after SARS-CoV-2 infection[26,27,58,59,66-68]. Though type I IFNs or MLL1 may each promote the expression of coagulopathy-associated factors[24], our finding that MLL1 suppresses *Ifna* expression indicates an alternate mechanism for coagulopathy in a setting of diminished IFN signaling after coronavirus infection. Importantly, our observation of MLL1 as a mediator of IFNα1-induced expression of coagulopathy-related factors in MO/Mφs may point to a role for MLL1 mediating IFN-dependent coagulopathy in other diseases such as sepsis. Nonetheless, additional studies are needed to delineate the relationship between MLL1 and global MO/Mφ transcription as attenuated expression of inflammatory cytokines/coagulopathy-related factors after MLL1 loss may relate to a general decrease in transcription, with MLL1-*Ifna* regulation representing an exception to such a relationship.

Furthermore, an important role for CME and associated proteins continues to be described in the immunopathogenesis of SARS-CoV2 infection[28,29,69-72]. We observed rapid and sustained upregulation in MLL1 expression/function after coronavirus infection. Our finding that coronavirus-induced gene expression in MO/Mφs is abrogated by silencing MLL1 is interesting as it suggests that MLL1 activity may enforce “epigenetic memory”

after coronavirus infection, however what contribution MLL1-associated proteins/MLL1-complex components play in acute and chronic responses remains unclear. As such memory is thought to contribute to the long-term sequelae in conditions such as aging, malignancy, and after recovery from sepsis, it is possible a prolonged state of smoldering inflammation/dysregulated coagulation and other symptoms associated with "long-COVID"[69-71] may be mediated through "epigenetic memory".

The ability of CME and associated proteins to impact acute and chronic disease states renders factors such as MLL1 and its core components (e.g., Menin, WDR5) as attractive therapeutic targets to blunt the sequalae of SARS-CoV-2 infection[38,40,42,73-77]. Targeting MLL1/MLL1 complexes with small molecule inhibitors has been described for MLL1-rearranged leukemia treatment[40,74], and such inhibitors may be used to target MLL1-driven CAC during which the balance between opposing procoagulant and fibrinolytic systems is perturbed. By addressing both hypercoagulability and hyperfibrinolysis, such therapies could prevent immunothrombosis/dysregulated fibrinolysis, and restore a normal coagulation profile without the attendant risks of current anticoagulant therapies, especially in the ICU patient population where bleeding risk of anticoagulants has been shown to outweigh the benefits[78]. Nonetheless, since MLL1 expression is not limited to MO/Mφs[37], it is unclear what effects would result from global inhibition of MLL1 activity (though immunosuppressive effects and poor wound healing a possible side-effects), and therefore MO/Mφs-targeted therapies must be designed. Furthermore, our experimental model of myeloid-specific MLL1 loss may capture MLL1's effects other cells of myeloid lineage, such as neutrophils, which have been implicated in SARS-CoV-2 pathogenesis, coagulopathy, and inflammatory response[79,80].

Our study highlights the potential role of MO/Mφ MLL1 in regulating coagulation/fibrinolysis and our findings add to the evidence that CMEs play major roles in directing MO/Mφ gene expression programs to drive micro/macrovascular immunopathology[32,42,81-85]. Epigenetics in translational thrombosis represents an exciting area of discovery that has the potential to uncover novel immune based therapeutic strategies in the study of vascular immunobiology. We have identified that MLL1 is a coronavirus-inducible factor in MO/Mφ that is responsible for the expression of inflammatory and coagulopathy-related gene expression. Our study shows that MO/Mφ MLL1 induces a hypercoagulable and fibrinolytic phenotype upon coronavirus infection. These results point to MLL1 blockade as a potential therapeutic strategy to curb coronavirus-associated coagulopathy and inflammation, and possible long-term sequelae associated with SARS-CoV-2 infection.

Acknowledgements:

We would like to acknowledge support from the Advanced Genomics Core and Bioinformatics Core of the University of Michigan Medical School's Biomedical Research Core Facilities and the Fredrick A. Coller Surgical Society. This work was supported by funding from the Vascular Cures Foundation (to A.T.O.), the Lefkofsky Family Foundation (to A.T.O.), the Elizabeth Anne Baiardi Research Fund (to A.T.O.), the University of Michigan Cardiovascular Center COVID igniter grant (to A.T.O.), the NIH/NIGMS (grant R35GM131835 to M.H.), the NIH/NCATS (grant R21TR003185 to M.H.), and the NIH/NHLBI (grants ZIAHL006267, ZIAHL006262, ZIAHL006263 to Y.K.; 5R01HL144550 to P.K.H.; 1K08HL155408-01 to A.T.O.). Finally, we would like to thank Lorie Gavulic for design of the visual abstract.

Authorship Contributions:

S.B.S., W.J.M., C.A.O., M.B., N.R., Y.K., J. S. K., R.A., M.H., B.B.M., P.K.H., T. W. W., K.A.G. and A.T.O. designed research strategy; S.B.S., W.J.M., C.O.A., M.B., N.R., and A.T.O. performed research; S.B.S., W.J.M., C.A.O., W.W., N.R., R.A., M.H., B.B.M, P.K.H, K.A.G., and A.T.O. contributed new reagents/analytic tools; W.W. performed analysis of sequencing data; S.B.S., W.J.M., C.A.O., N.R., R.A., M.H., B.B.M., T.W.W., P.K.H., K.A.G, and A.T.O. analyzed data; S.B.S and A.T.O. wrote the paper.

Conflict of Interest Disclosures:

M.H. is a consultant and equity holder for Veralox Therapeutics and a consultant for Cereno Scientific which has an option to license platelet inhibitory compounds from the University of Michigan. The authors do not declare any conflicts of interest.

References:

1. Giamarellos-Bourboulis EJ, Netea MG, Rovina N, et al. Complex Immune Dysregulation in COVID-19 Patients with Severe Respiratory Failure. *Cell Host Microbe*. 2020;27(6):992-1000 e1003.

2. Vanderbeke L, Van Mol P, Van Herck Y, et al. Monocyte-driven atypical cytokine storm and aberrant neutrophil activation as key mediators of COVID-19 disease severity. *Nat Commun*. 2021;12(1):4117.

3. Tang N, Li D, Wang X, Sun Z. Abnormal coagulation parameters are associated with poor prognosis in patients with novel coronavirus pneumonia. *J Thromb Haemost*. 2020;18(4):844-847.

418 4. Conway EM, Mackman N, Warren RQ, et al. Understanding COVID-19-associated coagulopathy. *Nature*
419 *Reviews Immunology*. 2022;22(10):639-649.
420 5. Cui S, Chen S, Li X, Liu S, Wang F. Prevalence of venous thromboembolism in patients with severe novel
421 coronavirus pneumonia. *J Thromb Haemost*. 2020;18(6):1421-1424.
422 6. Connors JM, Levy JH. COVID-19 and its implications for thrombosis and anticoagulation. *Blood*.
423 2020;135(23):2033-2040.
424 7. Levi M, Thachil J, Iba T, Levy JH. Coagulation abnormalities and thrombosis in patients with COVID-19. *Lancet*
425 *Haematol*. 2020;7(6):e438-e440.
426 8. D'Alonzo D, De Fenza M, Pavone V. COVID-19 and pneumonia: a role for the uPA/uPAR system. *Drug Discov*
427 *Today*. 2020;25(8):1528-1534.
428 9. Zhou F, Yu T, Du R, et al. Clinical course and risk factors for mortality of adult inpatients with COVID-19 in
429 Wuhan, China: a retrospective cohort study. *Lancet*. 2020;395(10229):1054-1062.
430 10. Wang D, Hu B, Hu C, et al. Clinical Characteristics of 138 Hospitalized Patients With 2019 Novel Coronavirus-
431 Infected Pneumonia in Wuhan, China. *JAMA*. 2020;323(11):1061-1069.
432 11. Chen N, Zhou M, Dong X, et al. Epidemiological and clinical characteristics of 99 cases of 2019 novel
433 coronavirus pneumonia in Wuhan, China: a descriptive study. *Lancet*. 2020;395(10223):507-513.
434 12. Guan WJ, Ni ZY, Hu Y, et al. Clinical Characteristics of Coronavirus Disease 2019 in China. *N Engl J Med*.
435 2020;382(18):1708-1720.
436 13. Page EM, Ariens RAS. Mechanisms of thrombosis and cardiovascular complications in COVID-19. *Thromb*
437 *Res*. 2021;200:1-8.
438 14. Iba T, Levy JH. Inflammation and thrombosis: roles of neutrophils, platelets and endothelial cells and their
439 interactions in thrombus formation during sepsis. *J Thromb Haemost*. 2018;16(2):231-241.
440 15. Nicolai L, Leunig A, Brambs S, et al. Immunothrombotic Dysregulation in COVID-19 Pneumonia Is Associated
441 With Respiratory Failure and Coagulopathy. *Circulation*. 2020;142(12):1176-1189.
442 16. Ruscitti P, Bruno F, Berardicurti O, et al. Lung involvement in macrophage activation syndrome and severe
443 COVID-19: results from a cross-sectional study to assess clinical, laboratory and artificial intelligence-radiological
444 differences. *Ann Rheum Dis*. 2020;79(9):1152-1155.

17. Humphries J, Gossage JA, Modarai B, et al. Monocyte urokinase-type plasminogen activator up-regulation reduces thrombus size in a model of venous thrombosis. *J Vasc Surg*. 2009;50(5):1127-1134.
18. Fleetwood AJ, Achuthan A, Schultz H, et al. Urokinase plasminogen activator is a central regulator of macrophage three-dimensional invasion, matrix degradation, and adhesion. *J Immunol*. 2014;192(8):3540-3547.
19. Scheibenbogen C, Moser H, Krause S, Andreesen R. Interferon-gamma-induced expression of tissue factor activity during human monocyte to macrophage maturation. *Haemostasis*. 1992;22(4):173-178.
20. Collins PW, Noble KE, Reittie JR, Hoffbrand AV, Pasi KJ, Yong KL. Induction of tissue factor expression in human monocyte/endothelium cocultures. *Br J Haematol*. 1995;91(4):963-970.
21. May AE, Schmidt R, Kanse SM, et al. Urokinase receptor surface expression regulates monocyte adhesion in acute myocardial infarction. *Blood*. 2002;100(10):3611-3617.
22. Dekkers PEP, Hove Tt, Velde AAt, Deventer SJHv, Poll Tvd. Upregulation of Monocyte Urokinase Plasminogen Activator Receptor during Human Endotoxemia. *Infection and Immunity*. 2000;68(4):2156-2160.
23. Rosell A, Havervall S, Meijenfeldt Fv, et al. Patients With COVID-19 Have Elevated Levels of Circulating Extracellular Vesicle Tissue Factor Activity That Is Associated With Severity and Mortality—Brief Report. *Arteriosclerosis, Thrombosis, and Vascular Biology*. 2021;41(2):878-882.
24. Wu S, Murrell GA, Wang Y. Interferon-alpha (Intron A) upregulates urokinase-type plasminogen activator receptor gene expression. *Cancer Immunol Immunother*. 2002;51(5):248-254.
25. Merad M, Martin JC. Pathological inflammation in patients with COVID-19: a key role for monocytes and macrophages. *Nature Reviews Immunology*. 2020;20(6):355-362.
26. Lee JS, Shin E-C. The type I interferon response in COVID-19: implications for treatment. *Nature Reviews Immunology*. 2020;20(10):585-586.
27. Galbraith MD, Kinning KT, Sullivan KD, et al. Specialized interferon action in COVID-19. *Proceedings of the National Academy of Sciences*. 2022;119(11):e2116730119.
28. Kgatle MM, Lawal IO, Mashabela G, et al. COVID-19 Is a Multi-Organ Aggressor: Epigenetic and Clinical Marks. *Front Immunol*. 2021;12:752380.
29. Melvin WJ, Audu CO, Davis FM, et al. Coronavirus induces diabetic macrophage-mediated inflammation via SETDB2. *Proc Natl Acad Sci U S A*. 2021;118(38).

30. Davis FM, denDekker A, Kimball A, et al. Epigenetic Regulation of TLR4 in Diabetic Macrophages Modulates Immunometabolism and Wound Repair. *J Immunol*. 2020;204(9):2503-2513.

31. Davis FM, Kimball A, denDekker A, et al. Histone Methylation Directs Myeloid TLR4 Expression and Regulates Wound Healing following Cutaneous Tissue Injury. *J Immunol*. 2019;202(6):1777-1785.

32. Kimball AS, Joshi A, Carson WFt, et al. The Histone Methyltransferase MLL1 Directs Macrophage-Mediated Inflammation in Wound Healing and Is Altered in a Murine Model of Obesity and Type 2 Diabetes. *Diabetes*. 2017;66(9):2459-2471.

33. Kuznetsova T, Prange KHM, Glass CK, de Winther MPJ. Transcriptional and epigenetic regulation of macrophages in atherosclerosis. *Nature Reviews Cardiology*. 2020;17(4):216-228.

34. Davis FM, Gallagher KA. Epigenetic Mechanisms in Monocytes/Macrophages Regulate Inflammation in Cardiometabolic and Vascular Disease. *Arteriosclerosis, Thrombosis, and Vascular Biology*. 2019;39(4):623-634.

35. Davis FM, Tsoi LC, Melvin WJ, et al. Inhibition of macrophage histone demethylase JMJD3 protects against abdominal aortic aneurysms. *J Exp Med*. 2021;218(6).

36. Davis FM, Schaller MA, Dendekker A, et al. Sepsis Induces Prolonged Epigenetic Modifications in Bone Marrow and Peripheral Macrophages Impairing Inflammation and Wound Healing. *Arterioscler Thromb Vasc Biol*. 2019;39(11):2353-2366.

37. Thul PJ, Åkesson L, Wiking M, et al. A subcellular map of the human proteome. *Science*. 2017;356(6340).

38. Alicea-Velázquez NL, Shinsky SA, Loh DM, Lee JH, Skalnik DG, Cosgrove MS. Targeted Disruption of the Interaction between WD-40 Repeat Protein 5 (WDR5) and Mixed Lineage Leukemia (MLL)/SET1 Family Proteins Specifically Inhibits MLL1 and SETd1A Methyltransferase Complexes. *J Biol Chem*. 2016;291(43):22357-22372.

39. Cao F, Townsend Elizabeth C, Karatas H, et al. Targeting MLL1 H3K4 Methyltransferase Activity in Mixed-Lineage Leukemia. *Molecular Cell*. 2014;53(2):247-261.

40. Borkin D, He S, Miao H, et al. Pharmacologic inhibition of the Menin-MLL interaction blocks progression of MLL leukemia in vivo. *Cancer Cell*. 2015;27(4):589-602.

41. Zhang P, Bergamin E, Couture JF. The many facets of MLL1 regulation. *Biopolymers*. 2013;99(2):136-145.

42. Xu J, Li L, Xiong J, et al. MLL1 and MLL1 fusion proteins have distinct functions in regulating leukemic transcription program. *Cell Discov*. 2016;2:16008.

43. Ansari KI, Kasiri S, Mandal SS. Histone methylase MLL1 has critical roles in tumor growth and angiogenesis and its knockdown suppresses tumor growth in vivo. *Oncogene*. 2013;32(28):3359-3370.

44. Grinat J, Heuberger J, Vidal RO, et al. The epigenetic regulator Mll1 is required for Wnt-driven intestinal tumorigenesis and cancer stemness. *Nat Commun*. 2020;11(1):6422.

45. Carson WFt, Cavassani KA, Soares EM, et al. The STAT4/MLL1 Epigenetic Axis Regulates the Antimicrobial Functions of Murine Macrophages. *J Immunol*. 2017;199(5):1865-1874.

46. Minotti R, Andersson A, Hottiger MO. ARTD1 Suppresses Interleukin 6 Expression by Repressing MLL1-Dependent Histone H3 Trimethylation. *Mol Cell Biol*. 2015;35(18):3189-3199.

47. Wang X, Zhu K, Li S, et al. MLL1, a H3K4 methyltransferase, regulates the TNFα-stimulated activation of genes downstream of NF-κB. *Journal of Cell Science*. 2012;125(17):4058-4066.

48. Hiscott J, Marois J, Garoufalis J, et al. Characterization of a functional NF-kappa B site in the human interleukin 1 beta promoter: evidence for a positive autoregulatory loop. *Mol Cell Biol*. 1993;13(10):6231-6240.

49. Libermann TA, Baltimore D. Activation of interleukin-6 gene expression through the NF-kappa B transcription factor. *Mol Cell Biol*. 1990;10(5):2327-2334.

50. Shakhov AN, Collart MA, Vassalli P, Nedospasov SA, Jongeneel CV. Kappa B-type enhancers are involved in lipopolysaccharide-mediated transcriptional activation of the tumor necrosis factor alpha gene in primary macrophages. *J Exp Med*. 1990;171(1):35-47.

51. Yang Z, Du J, Chen G, et al. Coronavirus MHV-A59 infects the lung and causes severe pneumonia in C57BL/6 mice. *Virol Sin*. 2014;29(6):393-402.

52. Hemmila E, Turbide C, Olson M, Jothy S, Holmes KV, Beauchemin N. Ceacam1a$^{-/-}$ Mice Are Completely Resistant to Infection by Murine Coronavirus Mouse Hepatitis Virus A59. *Journal of Virology*. 2004;78(18):10156-10165.

53. Blau DM, Turbide C, Tremblay M, et al. Targeted disruption of the Ceacam1 (MHVR) gene leads to reduced susceptibility of mice to mouse hepatitis virus infection. *J Virol*. 2001;75(17):8173-8186.

54. Del Valle DM, Kim-Schulze S, Huang HH, et al. An inflammatory cytokine signature predicts COVID-19 severity and survival. *Nat Med*. 2020;26(10):1636-1643.

55. Kyriazopoulou E, Huet T, Cavalli G, et al. Effect of anakinra on mortality in patients with COVID-19: a systematic review and patient-level meta-analysis. *Lancet Rheumatol*. 2021;3(10):e690-e697.

527 56. Kyriazopoulou E, Panagopoulos P, Metallidis S, et al. An open label trial of anakinra to prevent respiratory
528 failure in COVID-19. *Elife*. 2021;10.
529 57. Yang X, Cheng X, Tang Y, et al. The role of type 1 interferons in coagulation induced by gram-negative
530 bacteria. *Blood*. 2020;135(14):1087-1100.
531 58. Chua RL, Lukassen S, Trump S, et al. COVID-19 severity correlates with airway epithelium-immune cell
532 interactions identified by single-cell analysis. *Nat Biotechnol*. 2020;38(8):970-979.
533 59. Dalskov L, Møhlenberg M, Thyrsted J, et al. SARS-CoV-2 evades immune detection in alveolar macrophages.
534 *EMBO Rep*. 2020;21(12):e51252.
535 60. Hellum M, Franco-Lie I, Øvstebø R, Hauge T, Henriksson CE. The effect of corn trypsin inhibitor, anti-tissue
536 factor pathway inhibitor antibodies and phospholipids on microvesicle-associated thrombin generation in patients
537 with pancreatic cancer and healthy controls. *PLoS One*. 2017;12(9):e0184579.
538 61. Kirchhofer D, Moran P, Bullens S, Peale F, Bunting S. A monoclonal antibody that inhibits mouse tissue factor
539 function. *Journal of Thrombosis and Haemostasis*. 2005;3(5):1098-1099.
540 62. Zhang Q, Gupta S, Schipper DL, et al. NF-kappaB Dynamics Discriminate between TNF Doses in Single Cells.
541 *Cell Syst*. 2017;5(6):638-645 e635.
542 63. Cheng QJ, Ohta S, Sheu KM, et al. NF-kappaB dynamics determine the stimulus specificity of epigenomic
543 reprogramming in macrophages. *Science*. 2021;372(6548):1349-1353.
544 64. Wang G, Chen G, Zheng D, Cheng G, Tang H. PLP2 of mouse hepatitis virus A59 (MHV-A59) targets TBK1 to
545 negatively regulate cellular type I interferon signaling pathway. *PLoS One*. 2011;6(2):e17192.
546 65. Zhou H, Perlman S. Mouse hepatitis virus does not induce Beta interferon synthesis and does not inhibit its
547 induction by double-stranded RNA. *J Virol*. 2007;81(2):568-574.
548 66. Balkhi MY. Mechanistic understanding of innate and adaptive immune responses in SARS-CoV-2 infection.
549 *Mol Immunol*. 2021;135:268-275.
550 67. Pairo-Castineira E, Clohisey S, Klaric L, et al. Genetic mechanisms of critical illness in COVID-19. *Nature*.
551 2021;591(7848):92-98.
552 68. Tan Y, Tang F. SARS-CoV-2-mediated immune system activation and potential application in immunotherapy.
553 *Med Res Rev*. 2021;41(2):1167-1194.

554 69. Atlante S, Mongelli A, Barbi V, Martelli F, Farsetti A, Gaetano C. The epigenetic implication in coronavirus
555 infection and therapy. *Clin Epigenetics*. 2020;12(1):156.
556 70. Chlamydas S, Papavassiliou AG, Piperi C. Epigenetic mechanisms regulating COVID-19 infection. *Epigenetics*.
557 2021;16(3):263-270.
558 71. Corley MJ, Pang APS, Dody K, et al. Genome-wide DNA methylation profiling of peripheral blood reveals an
559 epigenetic signature associated with severe COVID-19. *J Leukoc Biol*. 2021;110(1):21-26.
560 72. Karwaciak I, Sałkowska A, Karaś K, Dastych J, Ratajewski M. Nucleocapsid and Spike Proteins of the
561 Coronavirus SARS-CoV-2 Induce IL6 in Monocytes and Macrophages-Potential Implications for Cytokine Storm
562 Syndrome. *Vaccines (Basel)*. 2021;9(1).
563 73. Dzama MM, Steiner M, Rausch J, et al. Synergistic Targeting of FLT3 Mutations in AML via Combined Menin-
564 MLL and FLT3 Inhibition. *Blood*. 2020.
565 74. Krivtsov AV, Evans K, Gadrey JY, et al. A Menin-MLL Inhibitor Induces Specific Chromatin Changes and
566 Eradicates Disease in Models of MLL-Rearranged Leukemia. *Cancer Cell*. 2019;36(6):660-673 e611.
567 75. Wang P, Lin C, Smith ER, et al. Global analysis of H3K4 methylation defines MLL family member targets and
568 points to a role for MLL1-mediated H3K4 methylation in the regulation of transcriptional initiation by RNA
569 polymerase II. *Mol Cell Biol*. 2009;29(22):6074-6085.
570 76. Li DD, Chen WL, Wang ZH, et al. High-affinity small molecular blockers of mixed lineage leukemia 1 (MLL1)-
571 WDR5 interaction inhibit MLL1 complex H3K4 methyltransferase activity. *Eur J Med Chem*. 2016;124:480-489.
572 77. Lu K, Tao H, Si X, Chen Q. The Histone H3 Lysine 4 Presenter WDR5 as an Oncogenic Protein and Novel
573 Epigenetic Target in Cancer. *Front Oncol*. 2018;8:502.
574 78. Investigators R-C, Investigators AC-a, Investigators A, et al. Therapeutic Anticoagulation with Heparin in
575 Critically Ill Patients with Covid-19. *N Engl J Med*. 2021;385(9):777-789.
576 79. Zuo Y, Yalavarthi S, Navaz SA, et al. Autoantibodies stabilize neutrophil extracellular traps in COVID-19. *JCI*
577 *Insight*. 2021;6(15).
578 80. McKenna E, Wubben R, Isaza-Correa JM, et al. Neutrophils in COVID-19: Not Innocent Bystanders. *Frontiers*
579 *in Immunology*. 2022;13.
580 81. Freson K, Izzi B, Van Geet C. From genetics to epigenetics in platelet research. *Thromb Res*. 2012;129(3):325-
581 329.

582 82. Pandey D, Sikka G, Bergman Y, et al. Transcriptional regulation of endothelial arginase 2 by histone deacetylase
583 2. *Arterioscler Thromb Vasc Biol*. 2014;34(7):1556-1566.
584 83. Kaluza D, Kroll J, Gesierich S, et al. Histone deacetylase 9 promotes angiogenesis by targeting the
585 antiangiogenic microRNA-17-92 cluster in endothelial cells. *Arterioscler Thromb Vasc Biol*. 2013;33(3):533-543.
586 84. Greissel A, Culmes M, Burgkart R, et al. Histone acetylation and methylation significantly change with severity
587 of atherosclerosis in human carotid plaques. *Cardiovasc Pathol*. 2016;25(2):79-86.
588 85. Li Y, Reddy MA, Miao F, et al. Role of the histone H3 lysine 4 methyltransferase, SET7/9, in the regulation of
589 NF-kappaB-dependent inflammatory genes. Relevance to diabetes and inflammation. *J Biol Chem*.
590 2008;283(39):26771-26781.

591 **Figure Legends:**

592 **Figure 1: Coronavirus infection of MO/Mφs induces expression of MLL1, coagulopathy-related factors and**
593 **inflammatory cytokines.** Bone marrow derived macrophages were harvested from C57Bl6/J mice (WT-BMDMs)
594 and were infected with 1 MOI of the murine coronavirus MHVA59 for the indicated times and mRNA (A) and
595 protein levels (B; representative blot shown [β-actin served as loading control]) of *Kmt2a/*MLL1 were assayed by
596 qRT-PCR and immunoblotting, respectively. (C) mRNA levels of factors important in CAC (*Plau*, *Plaur*, and *F3*)
597 were measured in infected BMDMs. (D) mRNA levels of proinflammatory cytokines identified in the inflammatory
598 signature resulting from acute SARS-CoV-2 (IL6 and TNFα) and the MLL1 regulated cytokine IL1β were measured
599 in infected BMDMs. (E and F) Protein levels of coagulopathy-related factors (E) and proinflammatory cytokines (F)
600 were assayed by ELISA. Bar graphs represent mean values from at least n=5 independent experiments assayed in
601 triplicate and individual data points represent independent experiments. Errors bars represent standard error (SE).
602 Statistical testing was performed using Kruskal-Wallis tests with corrections for multiple comparisons. * $p < 0.05$;
603 ** $p < 0.01$; *** $p < 0.001$; **** $p < 0.0001$.

604 **Figure 2: MLL1 regulates the basal expression of coagulopathy-related factors and proinflammatory**
605 **cytokines in BMDMs.** BMDMs were harvested from mice carrying a myeloid specific deletion of MLL1 (*Kmt2a*$^{fl/fl}$
606 Lyz2Cre$^{+/-}$; denoted Cre+) and littermate controls (*Kmt2a*$^{fl/fl}$ Lyz2Cre$^{-/-}$; denoted Cre-). (A) mRNA levels of *Kmt2a*
607 were assayed in n=8 Cre+ and Cre- animals analyzed in triplicate. (B) Protein levels of MLL1 were assayed in
608 BMDMs from n=4 Cre+ and Cre- mice by immunoblotting (representative blot shown [β-actin served as loading

609 control]. (C and D) mRNA levels of coagulopathy-related factors (C) and proinflammatory cytokines (D) was
610 assayed. (E and F) Protein levels of coagulopathy-related factors (E) and inflammatory cytokines (F) were measured
611 by ELISA. (G) Chromatin immunoprecipitation (ChIP) assays were performed using antibodies specific to either
612 H3K4me3 or non-targeting species specific IgG. Bars graphs represent mean values from at least n=4 independent
613 experiments with individual data points representing independent experiments. For ChIP experiments, bar graphs
614 represent mean ChIP intensity relative to IgG derived from n=8 samples performed in triplicate. Statistical analysis
615 of pairwise comparisons was performed using Mann-Whitney tests. Error bars represent standard error (SE). * $p <$
616 0.05; ** $p < 0.01$; *** $p < 0.001$; **** $p < 0.0001$.

617 **Figure 3: Loss of MLL1 attenuates coronavirus and proinflammatory cytokine mediated induction of**
618 **coagulopathy-related factors and proinflammatory cytokines in BMDMs.** BMDMs were harvested from mice
619 carrying a myeloid specific deletion of MLL1 (*Kmt2a*$^{fl/fl}$ Lyz2Cre$^{+/-}$; denoted Cre+) and littermate controls (*Kmt2a*$^{fl/fl}$
620 Lyz2Cre$^{-/-}$; denoted Cre-). Cells were either stimulated with TNFα (5 ng/ml), IL1β (5 ng/ml), or IL6 (5 ng/ml) or
621 infected with 1 MOI of MHVA59 for 24 hours. (A and B) mRNA levels of coagulopathy associated factors and
622 inflammatory cytokines were assayed in stimulated/infected cells were assayed by qRT-PCR. (C and D) Protein
623 levels of coagulopathy-related factors (C) and inflammatory cytokines (D) were measured by ELISA. Crossed
624 circles indicate cytokine which was not measured in each assay as the particular cytokine was used for stimulation.
625 (E) ChIP assays were performed using antibodies specific for H3K4me3 or with non-targeting species specific IgG
626 antibodies. ChIP intensity (relative to IgG) at the indicated promoters is shown. For qRT-PCR and ELISA
627 experiments, graphs feature results from n=10 animals assayed in triplicate. For ChIP experiments, bar graphs
628 represent mean ChIP intensity relative to IgG from n=8 animals assayed in triplicate. Error bars represent standard
629 error (SE). For clarity of figure, graphical representation of statistical significance is not shown. Statistical analysis
630 of datasets was performed using Mann-Whitney U tests and pairwise comparisons between Cre- and Cre+ cells were
631 found to meet criteria for statistical significance ($p < 0.05$) except where indicated.

632 **Figure 4: MLL1 is required for RelA-dependent transcription of coagulopathy associated factors.** (A) *Rela*
633 mRNA levels were assayed in BMDMs harvested from MLL1 knockout mice (Cre+; n=4) and littermate controls
634 (Cre-; n=4). (B) RelA protein levels are assayed in these cells by immunoblot (β-actin served as loading control).
635 (C) The protein expression of MLL1 (MLL1^{C} = C-terminal epitope), phospho-RelA (Ser536), and RelA was assayed

in RAW264.7 cells that were transfected with either of two distinct siRNAs targeting MLL1 (denoted -1 and -2) or a non-targeting control (-Ctl). (β-actin served as loading control) (D) mRNA expression of *Rela* and *Kmt2a* was assayed in BMDMs transfected with siRNAs targeting *Rela* (smartpool; denoted siRelA) or a non-targeting control (siCtl). Results are representative of n=4 independent experiments assayed in triplicate (E) Protein levels of MLL1 and RelA were assayed and representative immunoblot is shown. (F) BMDMs from littermate control mice (n=8, assayed in triplicate) were transfected with the siRNAs were infected with 1 MOI of MHVA59 for 24 hours and mRNA levels of *Kmt2a* were measured. (G) Cre- and Cre+ BMDMs (n=7 per group; assayed in triplicate) were transfected as indicated and infected with 1 MOI of MHVA59 for 24 hours and mRNA levels of *Rela* were assayed in these cells. (H) Cre- and Cre+ BMDMs (n=7 per group; assayed in triplicate) were infected with MHVA59 for the indicated duration and ChIP assays were performed with antibodies specific to RelA or IgG. (I) mRNA levels of coagulopathy associated factors were assayed in the indicated transfected cells (n=7; performed in triplicate). (J) Protein levels of these coagulopathy-related factors were measured by ELISA (n=7; performed in triplicate). (K) RelA ChIP assays were performed on candidate promoters and ChIP intensity relative to IgG was measured at the indicated promoters (n=7 per group; assayed in triplicate). Bar graphs represent mean values and error bars represent standard error (SE). Statistical analysis was performed by either Mann-Whitney U-test or Kruskal-Wallis test with corrections for multiple comparisons. Error bars represent standard error (SE). * $p < 0.05$; ** $p < 0.01$; *** $p < 0.001$; **** $p < 0.0001$.

Figure 5: Coronavirus induces the expression of MLL1 and its associated factors in MO/Mφs *in vivo* and promotes a prothrombotic and profibrinolytic phenotype. C57BL6/J mice underwent intranasal inoculation of $2x10^5$ plaque forming units (*pfu*) MHVA59 (post-infection day 3 mice [d3; n=8]; post-infection day 28 mice [d28; n=9]) or PBS (denoted as sham; n=8). Mice were sacrificed at the indicated timepoints and plasma and splenic MO/Mφs (a surrogate for circulating MO/Mφs) were harvested. (A) *Kmt2a* mRNA levels were assayed by qRT-PCR. (B and C) The mRNA levels and protein levels of coagulopathy associated factors in splenic MO/Mφs were measured by qRT-PCR and ELISA, respectively. (D) H3K4me3 abundance at the indicated promoters was assayed by ChIP assay. (E and F) Circulating levels of urokinase and urokinase receptor were measured by ELISA. (G) Plasma tissue factor protein levels was measured by ELISA. (H) Plasma urokinase activity levels were measured using a colorimetric assay in which absorbance (A405) correlates with enzyme activity level through the cleavage of a plasmin (activated by urokinase) substrate which liberates *p*-nitroaniline. (I) Plasma tissue factor activity was

measured using a colorimetric assay in which the activation of factor X (FXa) by tissue factor and factor VII (TF/FVIIa) and its cleavage of a FXa specific substrate liberates *p*-nitroaniline. (J) The tissue factor activity of lysed harvested splenic MO/Mφs was measured. (K) Tail vein bleeding time was measured in infected and sham mice. (L) The number of re-bleeding events during tail vein bleeding time assays was tallied. (M) Whole blood was collected from infected and sham mice by inferior vena cava puncture and anticoagulated with 3.2 % sodium citrate at a ratio of 9:1 (blood to citrate). Thromboelastography (TEG) was performed and R-time (time to formation of clot of 2 mm thickness) was measured (left panel). Representative TEGs are presented in the right panel. (N) To determine the role of tissue factor in hypercoagulability as assayed by a shortened R-time as measured by TEG after coronavirus infection, citrated whole blood samples from either sham or infected (d3) mice was treated with either corn trypsin inhibitor (CTI; 25 μg/ml final concentration) or a mouse specific anti-tissue factor neutralizing antibody (TFI; clone 1H1 [Genentech]; 50 μg/ml final concentration) and the resultant viscoelastic properties were analyzed using TEG. Samples which were not subjected to treatment (NT) served as controls. Bar graphs represent mean values. qRT-PCR, ELISA, and ChIP data represent experiments performed in triplicate. Error bars represent standard error (SE). Statistical analysis of datasets were performed by either Mann-Whitney U-test or Kruskal-Wallis test with corrections for multiple comparisons. * $p < 0.05$; ** $p < 0.01$; *** $p < 0.001$; **** $p < 0.0001$.

Figure 6: Coronavirus-mediated induction of coagulopathy-related factors and the resultant coagulopathy is dependent on myeloid-specific expression of MLL1. Mice harboring a myeloid specific MLL1 knockout (denoted Cre+; n indicated per group) and littermate controls (Cre-) underwent intranasal inoculation of $2x10^5$ plaque forming units (*pfu*) of MHVA59. Mice were sacrificed at the indicated timepoints and plasma and splenic MO/Mφs (a surrogate for circulating MO/Mφs) were harvested. (A and B) The mRNA and protein levels of coagulation associated factors were assayed by qRT-PCR and ELISA in splenic MO/Mφs, respectively. (C) H3K4me3 abundance at the indicated promoters was measured by ChIP assay. (D and E) Circulating levels of urokinase (D) and soluble urokinase receptor (E) were measured by ELISA. (F) Plasma urokinase activity levels were measured using a colorimetric assay in which absorbance (A405) correlates with enzyme activity level through the cleavage of a plasmin (activated by urokinase) substrate which liberates *p*-nitroaniline. (G) Plasma tissue factor protein levels was measured by ELISA. (H) Plasma tissue factor activity was measured using a colorimetric assay in which the activation of factor X (FXa) by tissue factor and factor VII (TF/FVIIa) and its cleavage of a FXa specific substrate liberates *p*-nitroaniline. (I) The tissue factor activity of lysed harvested splenic MO/Mφs was measured. (J) Tail vein

bleeding time was measured in infected and sham mice. (K) The number of re-bleeding events during tail vein bleeding time assays was tallied. (L) Whole blood was collected from infected and sham mice by inferior vena cava puncture and anticoagulated with 3.2 % sodium citrate at a ratio of 9:1 (blood to citrate). TEG was performed and R-time (time to formation of clot of 2 mm thickness) was measured (left panel). Representative TEG is presented in the right panel. (M) To determine the role of tissue factor in hypercoagulability as assayed by a shortened R-time as measured by TEG after coronavirus infection, citrated whole blood samples from either infected (d3) Cre- or Cre+ mice was treated with either corn trypsin inhibitor (CTI; 25 μg/ml final concentration) or a mouse specific anti-tissue factor neutralizing antibody (TFI; clone 1H1 [Genentech]; 50 μg/ml final concentration) and the resultant viscoelastic properties were analyzed using TEG. Samples which were not subjected to treatment (NT) served as controls. Representative TEG is presented in the right panel. Bar graphs represent mean values and number of independent experiments per panel is as indicated. qRT-PCR, ELISA, and ChIP experiments were performed in triplicate. Error bars represent standard error (SE). Statistical comparisons were performed by either Mann-Whitney U-test or Kruskal-Wallis test with corrections for multiple comparisons. * $p < 0.05$; ** $p < 0.01$; *** $p < 0.001$; **** $p < 0.0001$.

Figure 7: SARS-CoV-2 infected patients display elevated levels of MLL1 in MO/Mφs, and upregulated expression of MO/Mφ and circulating coagulopathy associated factors and inflammatory cytokines. $CD14^+$ cells were isolated peripheral blood samples from hospitalized SARS-CoV-2 infected patients (hCOV+; n=28), hospitalized COVID negative patients (hCOV-; n=24), and healthy controls (n=14). (A) The mRNA levels of *KMT2A* were measured in isolated cells by qRT-PCR. (B and C) The mRNA and protein levels of coagulopathy associated factors in MO/Mφs were assayed by qRT-PCR and ELISA, respectively. (D) The expression of coagulopathy associated factors was measured from isolated plasma samples. (E) H3K4me3 and (F) MLL1 abundance at the indicated promoters was measured by ChIP assay. (G) Plasma urokinase activity was measured using a colorimetric assay in which absorbance (A405) correlates with enzyme activity level through the cleavage of a plasmin (activated by urokinase) substrate which liberates *p*-nitroaniline. (H) Plasma tissue factor activity was measured using a colorimetric assay in which the activation of factor X (FXa) by tissue factor and factor VII (TF/FVIIa) and its cleavage of a FXa specific substrate liberates *p*-nitroaniline. (M) Schematic of the proposed mechanism of coronavirus virus induced inflammation and coagulopathy as mediated by MLL1 in MO/Mφs. Bar graphs represent mean values. qRT-PCR, ELISA, and ChIP experiments were performed in triplicate. Error bars

represent standard error (SE). Statistical comparisons were performed using the Kruskal-Wallis test with corrections for multiple comparisons. * $p < 0.05$; ** $p < 0.01$; *** $p < 0.001$; **** $p < 0.0001$.

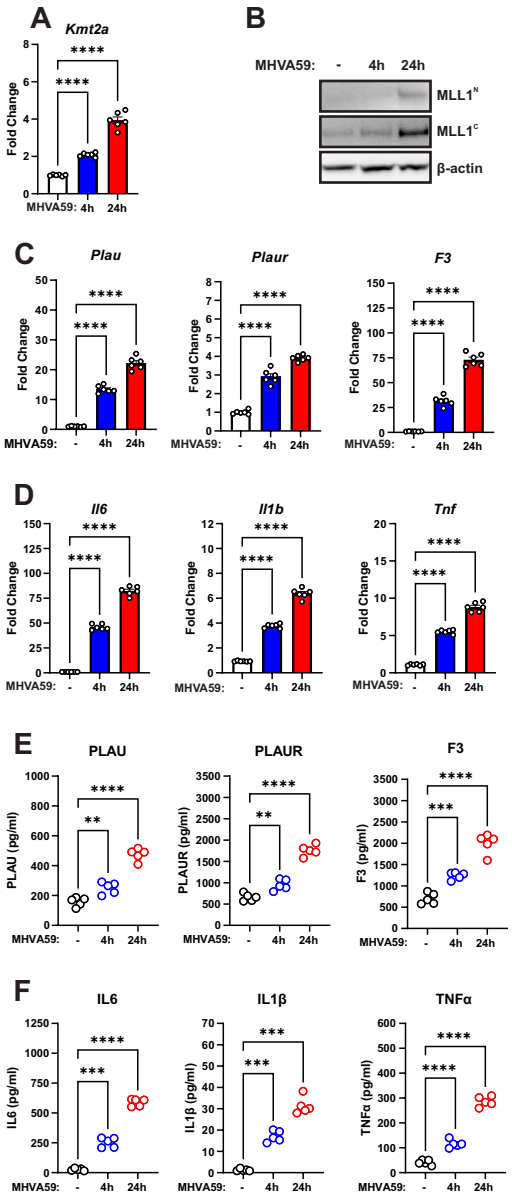
A
Kmt2a
Fold Change
MHVA59: 4h 24h
B
MHVA59: - 4h 24h
MLL1N
MLL1C
β-actin
C
Plau
Plaur
F3
Fold Change
MHVA59: - 4h 24h
D
Il6
Il1b
Tnf
Fold Change
MHVA59: - 4h 24h
E
PLAU
PLAUR
F3
PLAU (pg/ml)
PLAUR (pg/ml)
F3 (pg/ml)
MHVA59: - 4h 24h
F
IL6
IL1β
TNFα
IL6 (pg/ml)
IL1β (pg/ml)
TNFα (pg/ml)
MHVA59: - 4h 24h

Figure 1

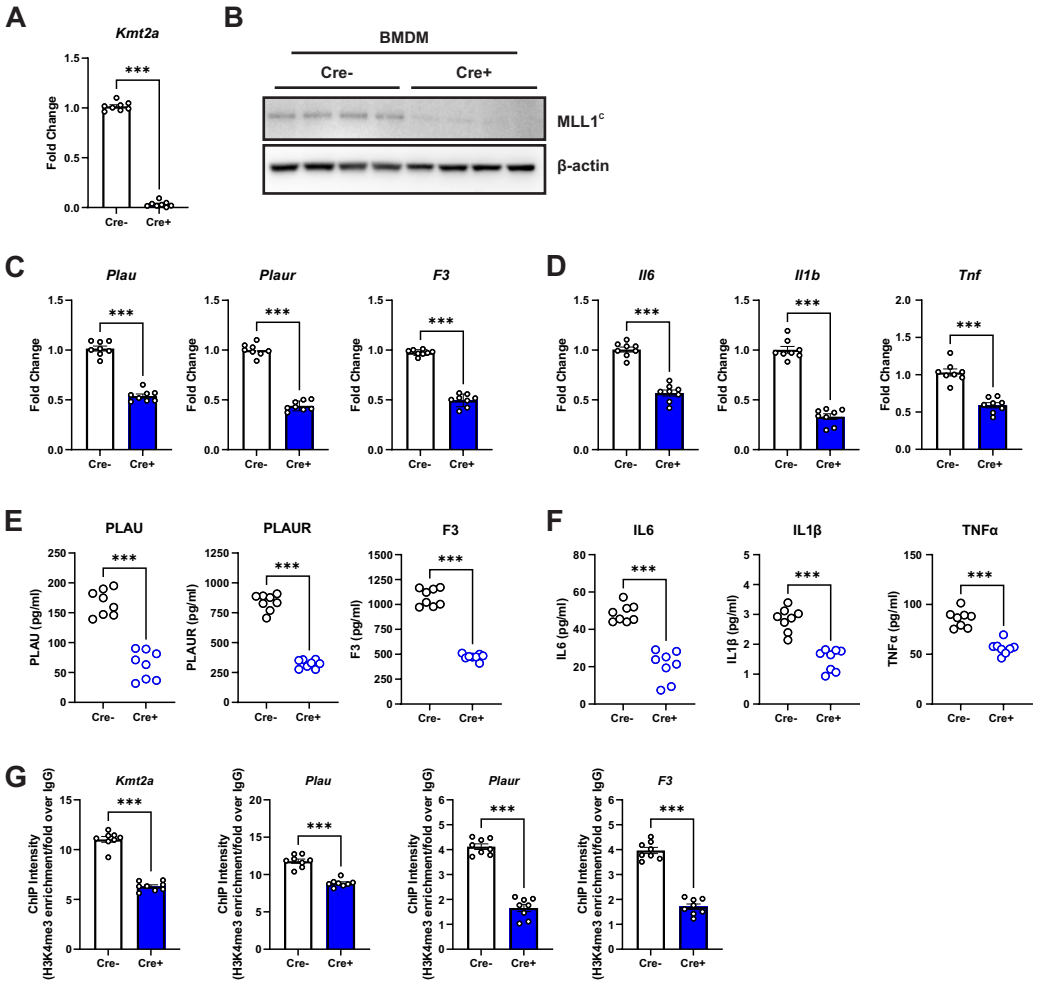
A
Kmt2a
Fold Change
***
Cre-
Cre+
B
BMDM
Cre-
Cre+
MLL1^c
β-actin
C
Plau
Plaur
F3
D
Il6
Il1b
Tnf
E
PLAU
PLAUR
F3
PLAU (pg/ml)
PLAUR (pg/ml)
F3 (pg/ml)
F
IL6
IL1β
TNFα
IL6 (pg/ml)
IL1β (pg/ml)
TNFα (pg/ml)
G
Kmt2a
Plau
Plaur
F3
ChIP Intensity (H3K4me3 enrichment/fold over IgG)

Figure 2

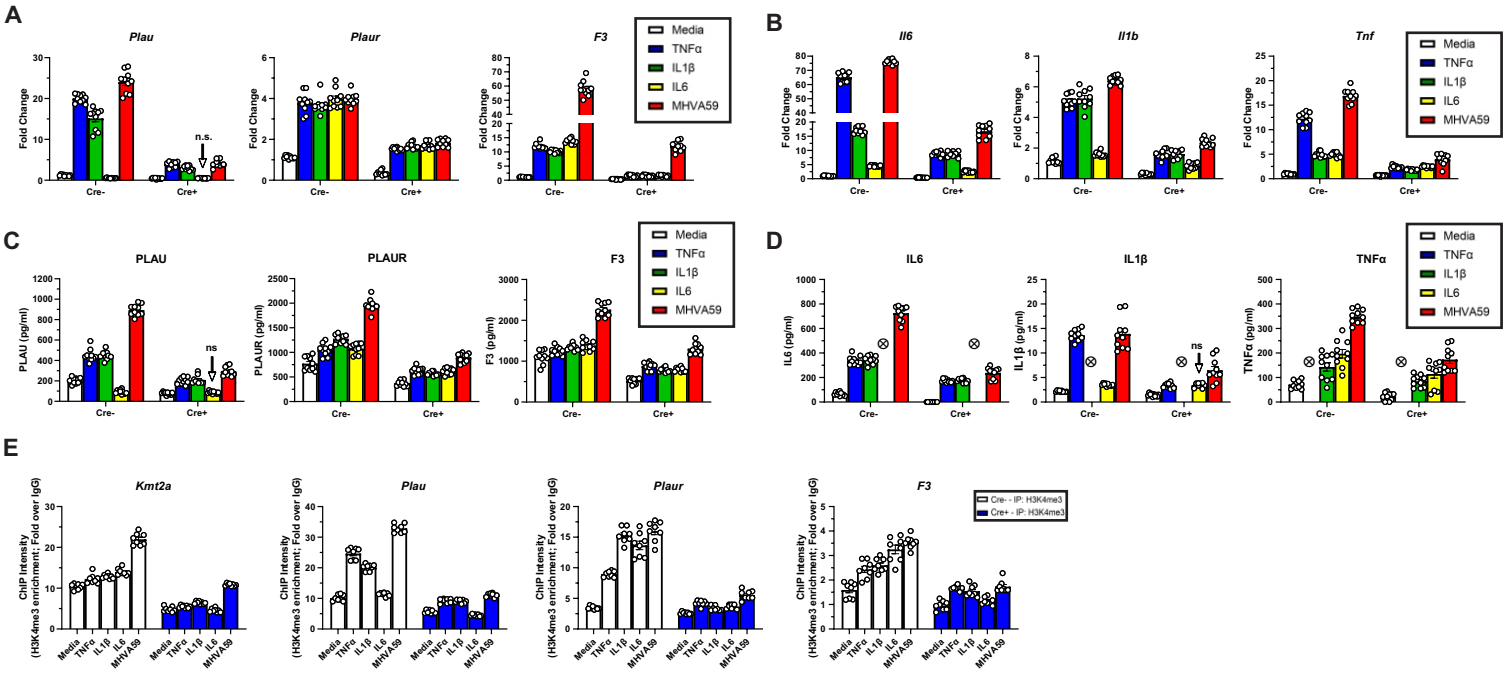
A
Plau
Plaur
F3
Fold Change
n.s.
Cre-
Cre+
Media
TNFα
IL1β
IL6
MHVA59
B
Il6
Il1b
Tnf
C
PLAU
PLAUR
F3
PLAU (pg/ml)
PLAUR (pg/ml)
F3 (pg/ml)
ns
D
IL6
IL1β
TNFα
IL6 (pg/ml)
IL1β (pg/ml)
TNFα (pg/ml)
E
Kmt2a
Plau
Plaur
F3
ChIP intensity (H3K4me3 enrichment; Fold over IgG)
Cre- - IP: H3K4me3
Cre+ - IP: H3K4me3

FIGURE 3

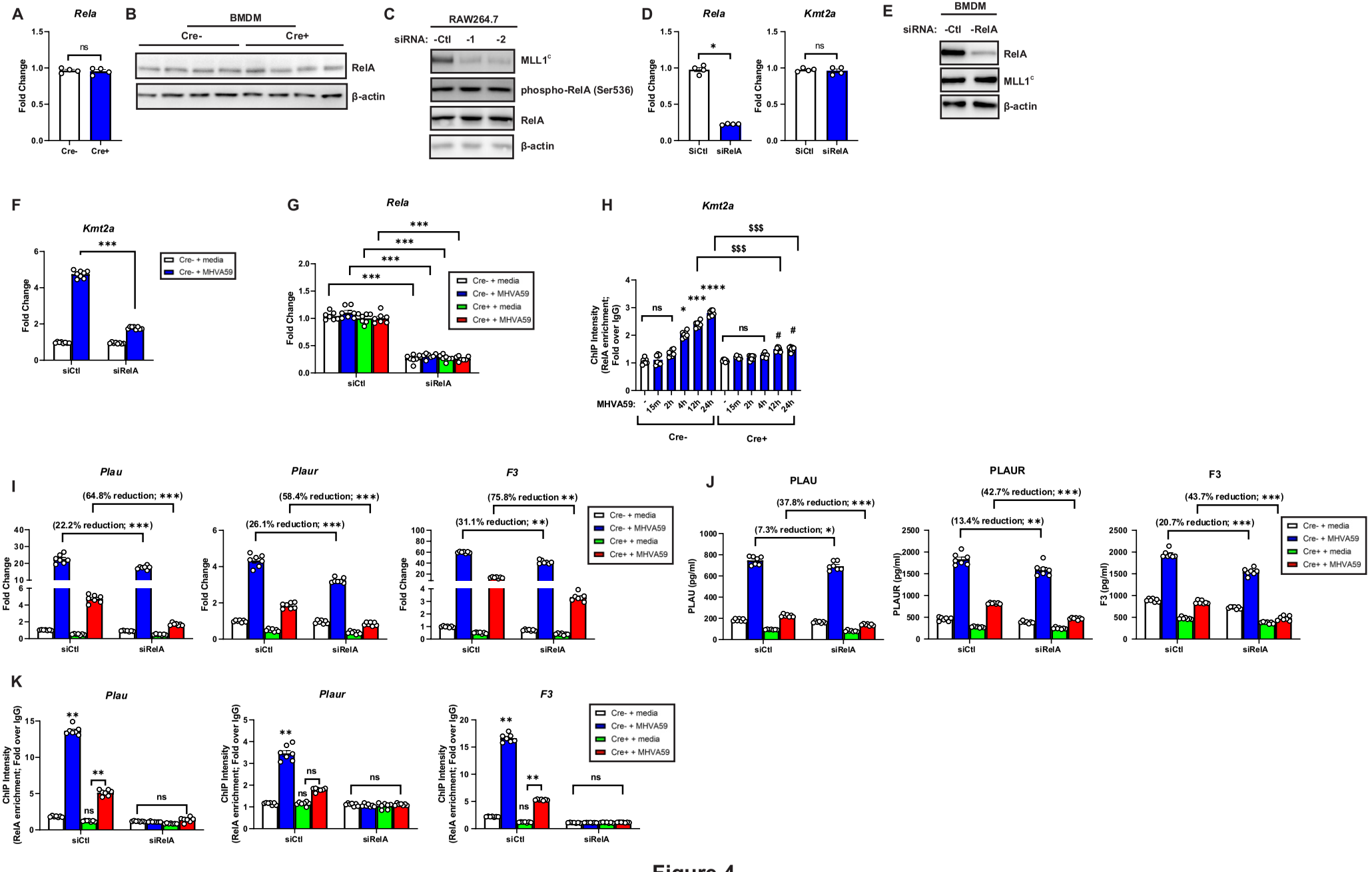
A
Rela
Fold Change
ns
Cre-
Cre+
B
BMDM
Cre-
Cre+
RelA
β-actin
C
RAW264.7
siRNA: -Ctl -1 -2
MLL1^c
phospho-RelA (Ser536)
RelA
β-actin
D
Rela
Kmt2a
Fold Change
*
ns
SiCtl
siRelA
E
BMDM
siRNA: -Ctl -RelA
RelA
MLL1^c
β-actin
F
Kmt2a
Fold Change
***
Cre- + media
Cre- + MHVA59
siCtl
siRelA
G
Rela
Fold Change
***
Cre- + media
Cre- + MHVA59
Cre+ + media
Cre+ + MHVA59
siCtl
siRelA
H
Kmt2a
ChIP Intensity (RelA enrichment; Fold over IgG)
$$$
****
***
*
ns
#
MHVA59: - 15m 2h 4h 12h 24h - 15m 2h 4h 12h 24h
Cre-
Cre+
I
Plau
Plaur
F3
(64.8% reduction; ***)
(22.2% reduction; ***)
(58.4% reduction; ***)
(26.1% reduction; ***)
(75.8% reduction **)
(31.1% reduction; **)
Fold Change
siCtl
siRelA
Cre- + media
Cre- + MHVA59
Cre+ + media
Cre+ + MHVA59
J
PLAU
PLAUR
F3
(37.8% reduction; ***)
(7.3% reduction; *)
(42.7% reduction; ***)
(13.4% reduction; **)
(43.7% reduction; ***)
(20.7% reduction; ***)
PLAU (pg/ml)
PLAUR (pg/ml)
F3 (pg/ml)
K
Plau
Plaur
F3
ChIP Intensity (RelA enrichment; Fold over IgG)
**
ns
siCtl
siRelA
Cre- + media
Cre- + MHVA59
Cre+ + media
Cre+ + MHVA59

Figure 4

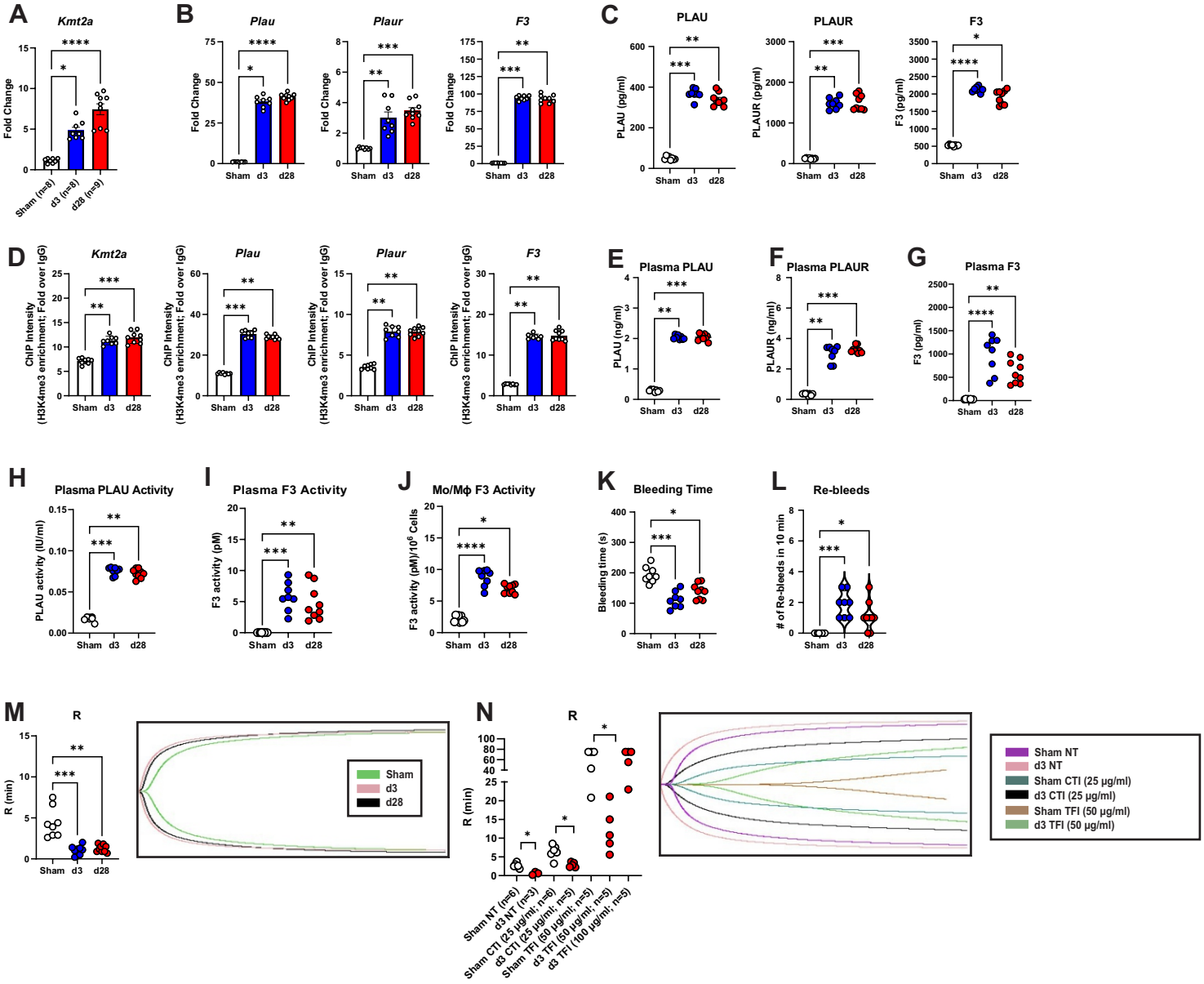
A
Kmt2a
Fold Change
Sham (n=8)
d3 (n=8)
d28 (n=9)
B
Plau
Plaur
F3
Fold Change
Sham d3 d28
C
PLAU
PLAUR
F3
PLAU (pg/ml)
PLAUR (pg/ml)
F3 (pg/ml)
D
Kmt2a
Plau
Plaur
F3
ChIP Intensity (H3K4me3 enrichment; Fold over IgG)
E
Plasma PLAU
PLAU (ng/ml)
F
Plasma PLAUR
PLAUR (ng/ml)
G
Plasma F3
F3 (pg/ml)
H
Plasma PLAU Activity
PLAU activity (IU/ml)
I
Plasma F3 Activity
F3 activity (pM)
J
Mo/Mϕ F3 Activity
F3 activity (pM)/10^6 Cells
K
Bleeding Time
Bleeding time (s)
L
Re-bleeds
# of Re-bleeds in 10 min
M
R
R (min)
Sham
d3
d28
N
R
R (min)
Sham NT (n=6)
d3 NT (n=3)
Sham CTI (25 µg/ml; n=6)
d3 CTI (25 µg/ml; n=5)
Sham TFI (50 µg/ml; n=5)
d3 TFI (50 µg/ml; n=5)
d3 TFI (100 µg/ml; n=5)
Sham NT
d3 NT
Sham CTI (25 µg/ml)
d3 CTI (25 µg/ml)
Sham TFI (50 µg/ml)
d3 TFI (50 µg/ml)

Figure 5

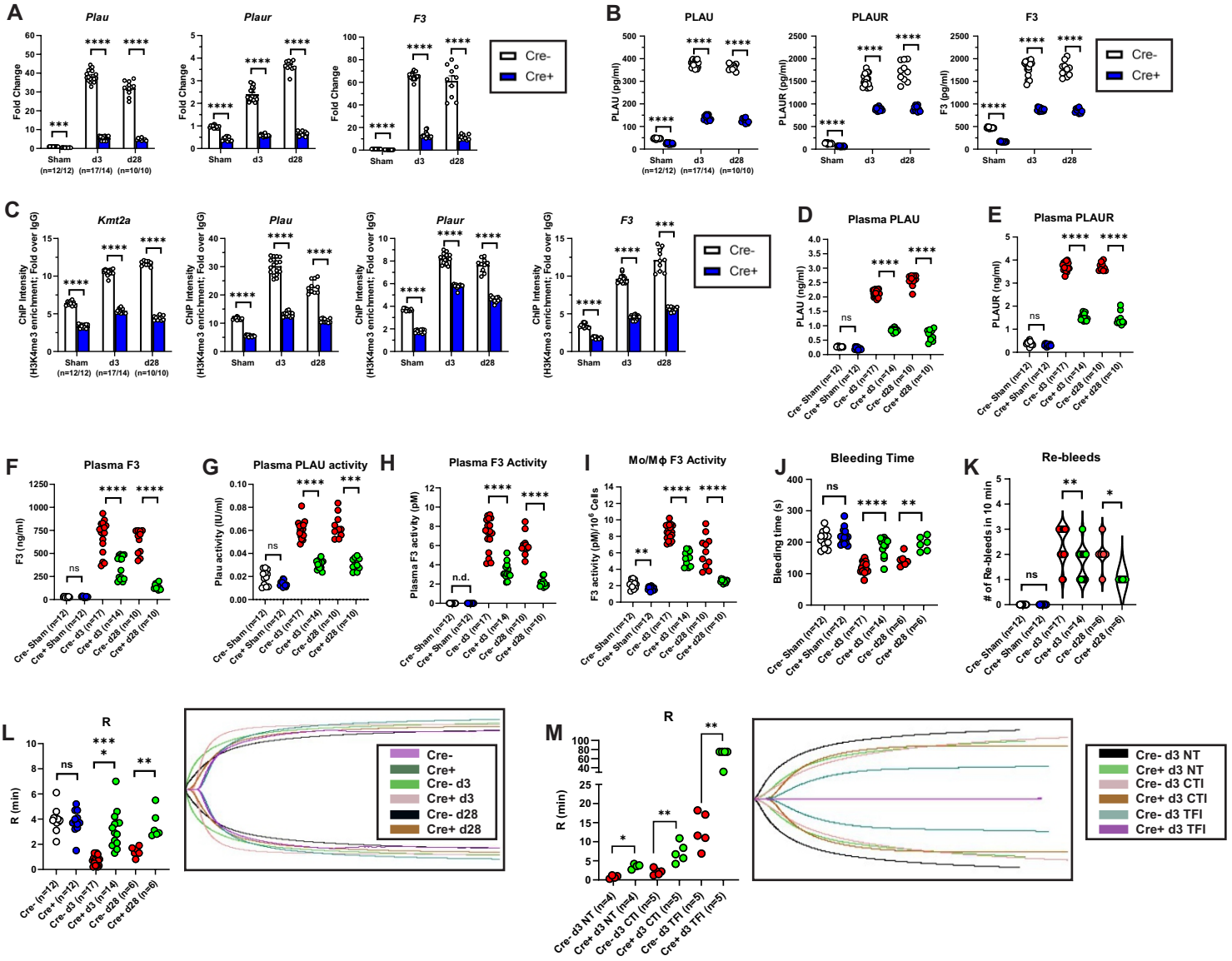
A
Plau
Plaur
F3
Fold Change
Cre-
Cre+
Sham
d3
d28
(n=12/12)
(n=17/14)
(n=10/10)
B
PLAU
PLAUR
F3
PLAU (pg/ml)
PLAUR (pg/ml)
F3 (pg/ml)
C
Kmt2a
Plau
Plaur
F3
ChIP Intensity (H3K4me3 enrichment; Fold over IgG)
D
Plasma PLAU
PLAU (ng/ml)
E
Plasma PLAUR
PLAUR (ng/ml)
F
Plasma F3
F3 (ng/ml)
G
Plasma PLAU activity
Plau activity (IU/ml)
H
Plasma F3 Activity
Plasma F3 activity (pM)
n.d.
I
Mo/Mϕ F3 Activity
F3 activity (pM)/10^6 Cells
J
Bleeding Time
Bleeding time (s)
K
Re-bleeds
# of Re-bleeds in 10 min
L
R
R (min)
Cre-
Cre+
Cre- d3
Cre+ d3
Cre- d28
Cre+ d28
M
R
R (min)
Cre- d3 NT (n=4)
Cre+ d3 NT (n=4)
Cre- d3 CTI (n=5)
Cre+ d3 CTI (n=5)
Cre- d3 TFI (n=5)
Cre+ d3 TFI (n=5)
Cre- d3 NT
Cre+ d3 NT
Cre- d3 CTI
Cre+ d3 CTI
Cre- d3 TFI
Cre+ d3 TFI

FIGURE 6

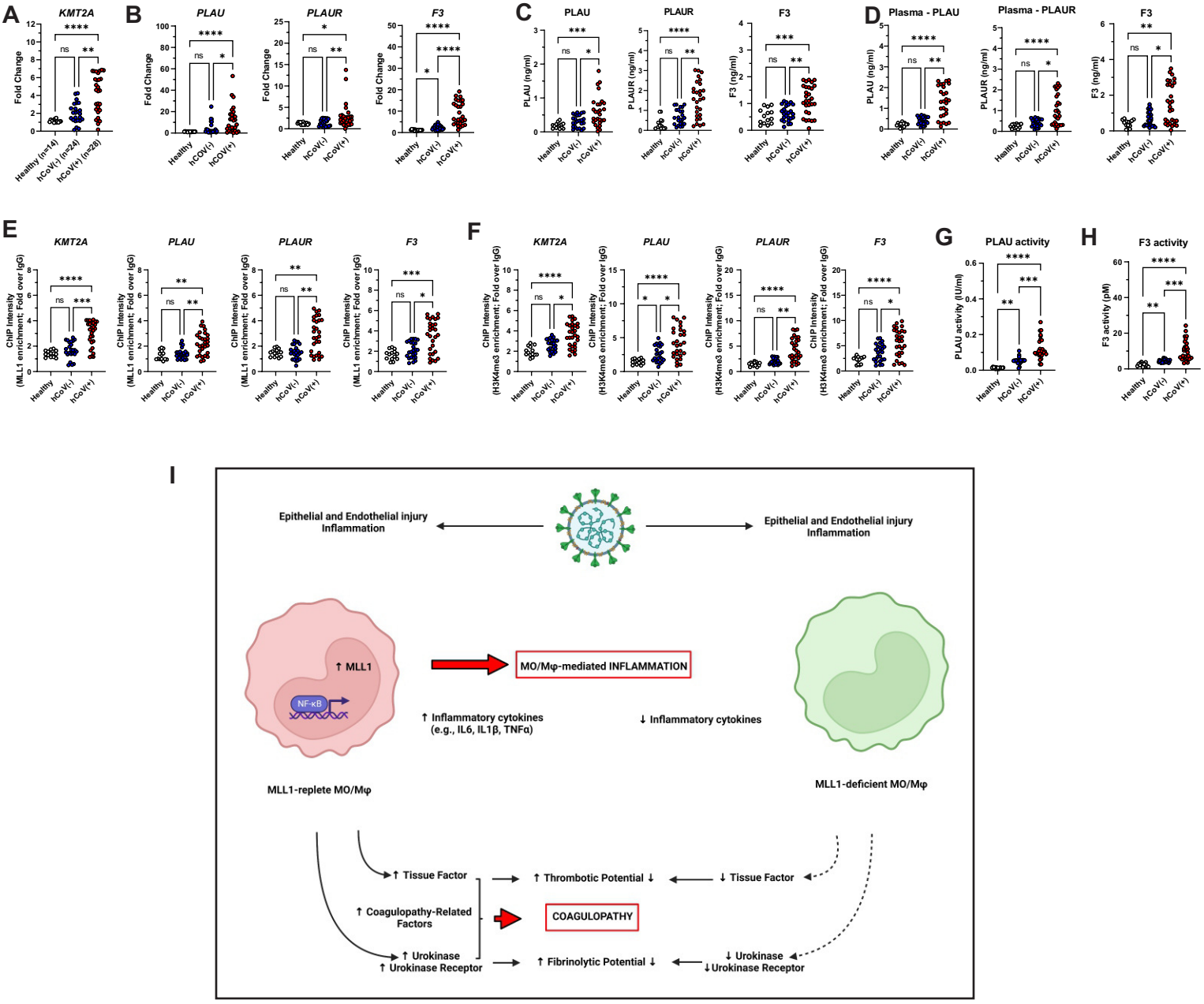
A
KMT2A
Fold Change
Healthy (n=14)
hCoV(-) (n=24)
hCoV(+) (n=28)
B
PLAU
PLAUR
F3
Fold Change
Healthy
hCoV(-)
hCoV(+)
C
PLAU
PLAUR
F3
PLAU (ng/ml)
PLAUR (ng/ml)
F3 (ng/ml)
D
Plasma - PLAU
Plasma - PLAUR
F3
E
KMT2A
PLAU
PLAUR
F3
ChIP Intensity (MLL1 enrichment; Fold over IgG)
F
KMT2A
PLAU
PLAUR
F3
ChIP Intensity (H3K4me3 enrichment; Fold over IgG)
G
PLAU activity
PLAU activity (IU/ml)
H
F3 activity
F3 activity (pM)
I
Epithelial and Endothelial injury
Inflammation
Epithelial and Endothelial injury
Inflammation
↑ MLL1
NF-κB
MO/Mφ-mediated INFLAMMATION
↑ Inflammatory cytokines
(e.g., IL6, IL1β, TNFα)
↓ Inflammatory cytokines
MLL1-replete MO/Mφ
MLL1-deficient MO/Mφ
↑ Tissue Factor
↑ Thrombotic Potential ↓
↓ Tissue Factor
↑ Coagulopathy-Related
Factors
COAGULOPATHY
↑ Urokinase
↑ Urokinase Receptor
↑ Fibrinolytic Potential ↓
↓ Urokinase
↓Urokinase Receptor